

## Divertor heat flux measurements in Globus-M

V.Yu. Sergeev<sup>1</sup>, A.S. Bykov<sup>1</sup>, N. A. Khromov<sup>2</sup>, V. K. Gusev<sup>2</sup>, B. V. Kuteev<sup>3</sup>, Yu. V. Petrov<sup>2</sup>,  
N.V. Sakharov<sup>2</sup>, S.V. Shatalin<sup>1</sup>, V.G. Skokov<sup>1</sup>, V.M. Timokhin<sup>1</sup>, S.Yu. Tolstyakov<sup>2</sup> and

F. Wagner<sup>1</sup>

<sup>1</sup>St. Petersburg State Polytechnical University, St. Petersburg, Russia

<sup>2</sup>Ioffe Physical Technical Institute, St. Petersburg, Russia

<sup>3</sup>RNC “Kurchatov Institute”, Moscow, Russia

**Introduction.** The limit on first wall and divertor heat loads is a main restriction of tokamak regimes because of high power densities. This is specifically critical for compact spherical tokamaks. The SOL heat flux width  $\lambda_q$  at the upstream point (normally at outer mid-plane) is a principal parameter determining heat loads onto the divertor plates at a given geometry and magnetic configuration. Since no first principle model exists for  $\lambda_q$  the evaluation is based on different scaling laws being established from experiments on spherical [1] or conventional [2] tokamaks or by heuristic approaches [3]. Globus-M is a compact spherical tokamak with high power density operating in different divertor magnetic configurations. It might be considered as a prototype of an FNS-ST (Fusion Neutron Source based on Spherical Tokamaks) whose design is presently in the conceptual stage [4]. The first measurements of the SOL heat flux width in Globus-M are presented here and compared with the scaling laws proposed for spherical tokamaks.

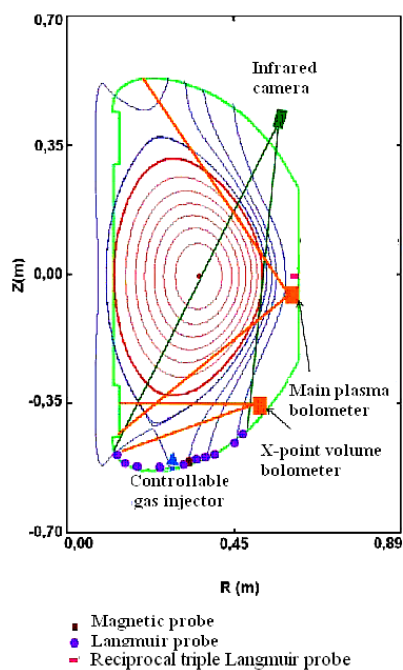


Fig 1. Experimental setup at Globus M.

**Experimental setup.** Several techniques were used to measure SOL plasma parameters in Globus-M as shown in Fig.1. Spatial distributions of the plasma density and electron temperature at lower divertor plates were measured by means of a set of ten flat Langmuir probes with a pin diameter of 8 mm. The temporal resolution of this diagnostics is about 2 ms and it is determined by the duration of measuring the current-voltage characteristics. A triple Langmuir probe provided density and electron temperature profiles (from shot to shot) at the outer mid-plane of the SOL. With a given sheath transmission coefficient the heat fluxes were evaluated. Additionally the heat flux distribution was measured at the lower

divertor plate using the infrared camera Gobi-384 [5]. This camera provides the temperature field over the divertor plates by measuring its radiation in the 8-14  $\mu\text{m}$  spectral range with spatial resolution of 1 mm, making 160 frames per second at 10  $\mu\text{s}$  exposure time. Heat fluxes onto the divertor plates were deduced from the measured surface temperatures of the divertor plates using a one-dimensional heat conduction model [6].

**Experimental results and discussion.** Measurements were performed in ohmically heated shots of Globus-M ( $a=24$  cm,  $R=36$  cm,  $k=1.8$ ,  $I_p=170$  kA,  $B_t(0)=0.4$  T,  $\langle n_e \rangle = 3.5 \times 10^{19} \text{ m}^{-3}$ ,  $T_e(0)=400$  eV,  $P_{OH}=300\text{-}350$  kW) in lower single null (LSN) and double null (DN) divertor configurations. Temporal evolutions of the plasma current, loop voltage, line-integrated density and radiation losses are shown in Fig. 2.

Profiles of heat fluxes onto the lower divertor plates measured by different diagnostics (continuous line from infrared data, diamonds from probes) at 183 ms (denoted by vertical lines in Fig. 2) during the steady-state stage of

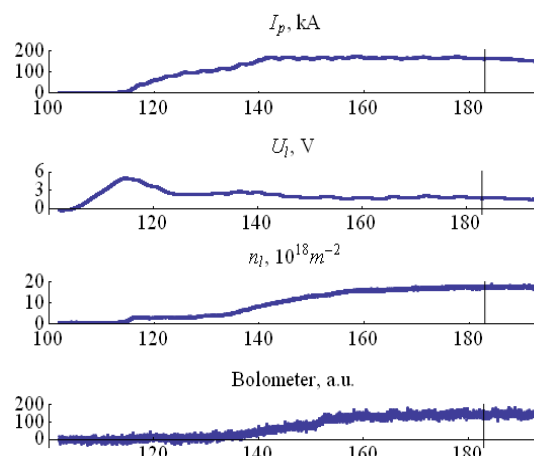


Fig. 2. Temporal evolutions of plasma parameters of Globus-M in experiments.

the discharge are compared in Fig. 3 for LSN and in Fig. 4 for DN magnetic configurations. The data of the triple Langmuir probe were mapped from the mid-plane using magnetic probes data and the magnetic flux map of the EFIT code [7]. It is seen from Fig. 3 that the infrared measured profile is in a good agreement with Langmuir probe data of the lower divertor plate. The maximum heat flux is about 1.2  $\text{MW}/\text{m}^2$  and the SOL width is about  $\lambda_{qdiv} \cong 15$  mm. A simple power balance for this OH LSN regime was carried out taking into account the measured low

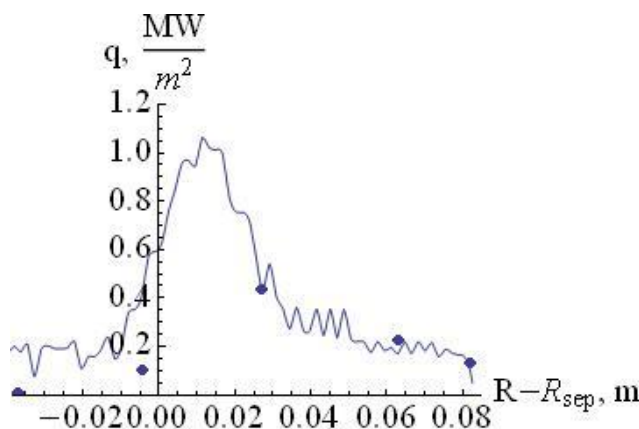


Fig. 3. Heat flux onto the lower divertor plate in LSN.

radiation losses ( $<10\%$ , see [7]) and a power distribution (9:1) between lower and upper divertors for the LSN configuration typical for spherical tokamaks [8]. Thus 260 kW heating power at 183 ms leads to about 190 kW power onto the lower divertor plate. The measured

power of about 90 kW is obtained by integration of the infrared profile as shown in Fig. 3. The observed difference might indicate that an essential part (about 50 %) of the power loss across the separatrix of Globus-M is transferred directly to the vacuum vessel walls.

For the DN configuration (Fig. 4) the maximum heat flux is about 0.4 MW/m<sup>2</sup> and the SOL width is about  $\lambda_{qdiv} \cong 20$  mm. Agreement between Langmuir probe data and infrared camera is also fairly good. The total power of 40 kW deposited onto the lower divertor plate is approximately half of the one measured for the LSN configuration which again is quite reasonable.

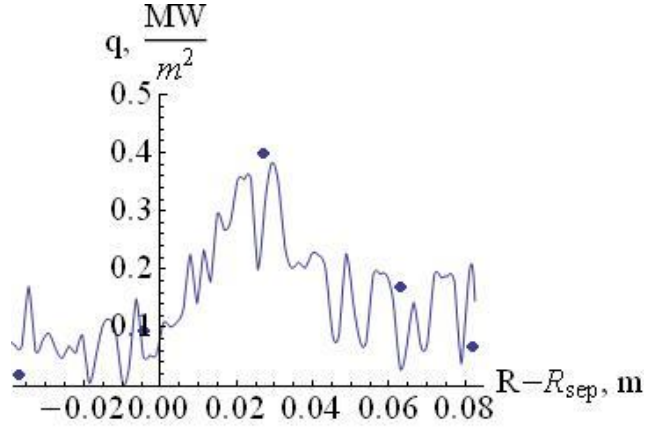


Fig. 4. Heat flux onto the lower divertor plate in DN.

For a comparison with scaling laws, the  $\lambda_{qdiv}$  values were mapped to the mid-plane SOL (“upstream”) position using EFIT and the following relationships of Ref. [9]:

$$\lambda_{qMP} = \frac{\lambda_{qdiv}}{\tilde{f}_{exp}}, \quad q_{MP} = \tilde{A}_{exp} q_{div}. \quad \text{Here, } \tilde{f}_{exp} = \frac{(B_{\theta}/B)_{MP}}{(B_{\theta}/B)_{div} \cos \alpha}, \quad \tilde{A}_{exp} = \tilde{f}_{exp} \frac{R_{div}}{R_{MP}}, \quad (B_{\theta}/B)_{MP} \text{ and}$$

$(B_{\theta}/B)_{div}$  are ratios of poloidal and total magnetic fields at the mid-plane and divertor plates, respectively;  $R_{MP}$  and  $R_{div}$  are the major radii of these points and  $\alpha$  is the angle between the magnetic field line and the normal to the divertor plate. The following parameters  $\tilde{A}_{exp} = 3$ ;  $\tilde{f}_{exp} = 5$  for LSN and  $\tilde{A}_{exp} = 2$ ;  $\tilde{f}_{exp} = 3$  for DN configurations were obtained for the data shown in Figs. 3 and 4.  $\lambda_{qMP} = 3\text{mm}$ ,  $q_{MP} = 6\text{MW}/\text{m}^2$  for the LSN and  $\lambda_{qMP} = 5\text{mm}$ ,  $q_{MP} = 1\text{MW}/\text{m}^2$  for DN configuration were obtained.

The measured  $\lambda_{qMP} = 3\text{-}5$  mm values are in fairly good agreement with those calculated from the scaling law of Ref. [3]  $\lambda_{qMP} = 2a\rho/R$ , which predicts  $\lambda_{qMP} = 4\text{-}6$  mm. Here,  $\rho$  is the poloidal Larmor ion radius at the “upstream” point. It should be noted that this scaling law also reproduces  $\lambda_{qMP}$  values measured in NSTX discharges [1]. These evaluations do not take into account a possible radial transport in the SOL and use data averaged over ELMs. This might be the reason why the recent scaling law [2] for the conventional tokamaks

deduced for the conditions between ELMs and taking into account radial transport predicts much lower decay length values for both Globus-M shots ( $\lambda_{qMP} = 1.4-1.6$  mm) presented here and for NSTX [1].

The scaling law of Ref. [3] predicts 2.5-3 mm of  $\lambda_{qMP}$  for FNS-ST basic mode operation [4] which is substantially lower than  $\lambda_{qMP} = 8$  mm assumed in Ref. [10] where the FNS-ST divertor operation was modeled. It also shows that the divertor heat flux at outer strike points in the DN divertor configuration of FNS-ST with 4-7 MW/m<sup>2</sup> might be underestimated by about a factor of 3 in Ref. [10]. Thus, the development of partially detached or even detached operation scenarios for the divertor might be required for the steady state operation of an FNS-ST.

**Conclusions.** Profiles of heat loads onto the lower divertor plate in LSN and DN divertor configurations of Globus-M have been measured by probes and an infrared camera; the two techniques demonstrate fairly good agreement. The data imply that the power onto the divertor plates is comparable to the one onto the vacuum vessel walls. The heat flux width values are in fairly good agreement with the scaling law that predicts this width being proportional to the poloidal Larmor ion radius at the “upstream” point and to the reversed aspect ratio of the machine.

**Acknowledgments.** This study was supported in part by the Ministry of Education and Science of the Russian Federation (contracts Nos. 11.G34.31.0041; 16.518.11.7003; 16.552.11.7002), the Russian Foundation for Basic Research (projects Nos. 11-08-1221a, 11-07-00567a).

## References.

- [1] R. Maingi et al. Proc. 34th EPS Conf. on Plas. Ph. Warsaw, 2007 ECA Vol.31F, P-2.020.
- [2] T. Eich et al. (2011) **107** PRL 215001.
- [3] R.J. Goldston et al. (2012) **52** Nucl. Fusion 013009.
- [4] B. V. Kuteev et al. (2011) **51** Nucl. Fusion 073013.
- [5] [http://www.xenics.com/en/infrared\\_camera/lwir-infrared\\_thermography\\_camera.asp](http://www.xenics.com/en/infrared_camera/lwir-infrared_thermography_camera.asp)
- [6] Carslaw and Jaeger, “Thermal conduction of solid bodies”, Oxford, 1959.
- [7] V.K. Gusev et al. (2009) **49** Nuclear Fusion 095022.
- [8] S.F. Paule et al. (2005) **337–339** Journal of Nuclear Materials 251–255.
- [9] P.C. Stangeby “The Plasma Boundary of Magnetic Fusion Devices”, Institute of Physics Publishing, Bristol and Philadelphia, 2004.
- [10] V. Yu. Sergeev et al. (2012) **38** Plasma Physics Reports 521–539.